Computer Simulation of Resistance Spot Welding in Aluminum: Part I

An electrothermal and mechanical model is developed to investigate the effects of process variables on the resistance spot welding of aluminum alloys

D. J. BROWNE, H. W. CHANDLER, J. T. EVANS AND J. WEN

ABSTRACT. A computer-based model of resistance spot welding with hemispherical electrode tips has been developed to include simulation of elastic-plastic mechanical deformation as well as ohmic heating and thermal conduction. The primary effect of the mechanical deformation is in its influence on the contact area and current density developed at the faying surface. The model was used to simulate spot welding in aluminum alloys. Preliminary results show the effects of variations in input current, contact resistance, applied force and position of the cooling water with respect to the electrode tip. It is shown that the value of the contact resistance has a large effect on nugget formation in the spot welding of aluminum alloys and that the applied force has a significant effect arising from its effect on the area of contact at the faying surface. The formation of a resistance spot weld in aluminum is also sensitive to the position of the cooling water-electrode interface because of the high thermal conductivity of aluminum alloys.

Introduction

Resistance spot welding has been used for many years as a reliable technique for joining pressed steel sheet. More recently, there has been an interest in the spot welding of aluminum alloy automotive structures and body shells. However, control of the spot welding of aluminum is often more difficult than of steel because of aluminum's higher electrical and thermal conductivities and lower melting point. In order to investigate the problem of forming a spot weld in aluminum, a model of the process was developed to study the interaction of variables with the ultimate aim of improving process control. The development of the model is described in this paper.

In resistance spot welding, two metal sheets are compressed between two water-cooled copper electrodes with an applied force P. Current is supplied to the sheets via the two electrodes to create concentrated heating at the faying surface. In spot welding steel, a current typically in the range 8 to 14 kA is required to form a good size nugget. In contrast, current in the range 20 to 30 kA is required to produce fusion in aluminum alloy sheets. Despite the simplicity of the underlying principles, there are many independent variables that can affect the spot welding process to a greater or lesser degree. Early attempts at modeling usually simplified the problem by considering it to be one-dimensional (Refs. 1–3), although one-dimensional models cannot predict the nugget diameter, which is of importance in determining the strength of the weld (Ref. 4). Two-dimensional finite difference models were developed (Refs. 5, 6) to make predictions of the nugget shape. By taking account of the change in materials properties with temperature and coupling the thermal and electrical aspects of the problem, Cho and Cho (Ref. 5) developed a model capable of accounting for fluctuations in localized heating, which is particularly important at the faying surface.

Finite element analysis has also been used to model spot welding, particularly when the mechanical aspects of the process have been investigated. Neid (Ref. 7) investigated the effect of the geometry of electrode and workpiece to predict the deformation and stresses as a function of temperature. However, the model was restricted to elastic deformation and did not calculate the contact areas at the electrode-sheet and faying surfaces. Kim and Eager (Ref. 8) investigated the effect of elastoplastic deformation using a coupled electro-thermal-mechanical finite element method. This model was limited to the treatment of a flat-ended electrode and did not treat the change in contact area with different applied forces, which occurs with conventional, domed electrodes. More recently, Tsai, *et al.* (Ref. 9), developed a coupled mechanical-electrothermal model which they used to produce weldability characteristic curves for steel sheet. Again, only flat-ended electrodes were modeled in

KEY WORDS

Computer Simulation
Resistance Spot Weld
Aluminum Alloys
Electrothermal Model
Mechanical Model
Process Variables
Applied Force
Mechanical Deformation
Contact Area
Current Density

H. W. CHANDLER, J. T. EVANS and J. WEN are with the Department of Mechanical, Materials and Manufacturing Engineering, University of Newcastle upon Tyne, Newcastle upon Tyne, U.K. D. J. BROWNE is with Alcan International, Banbury, Oxon, U.K.

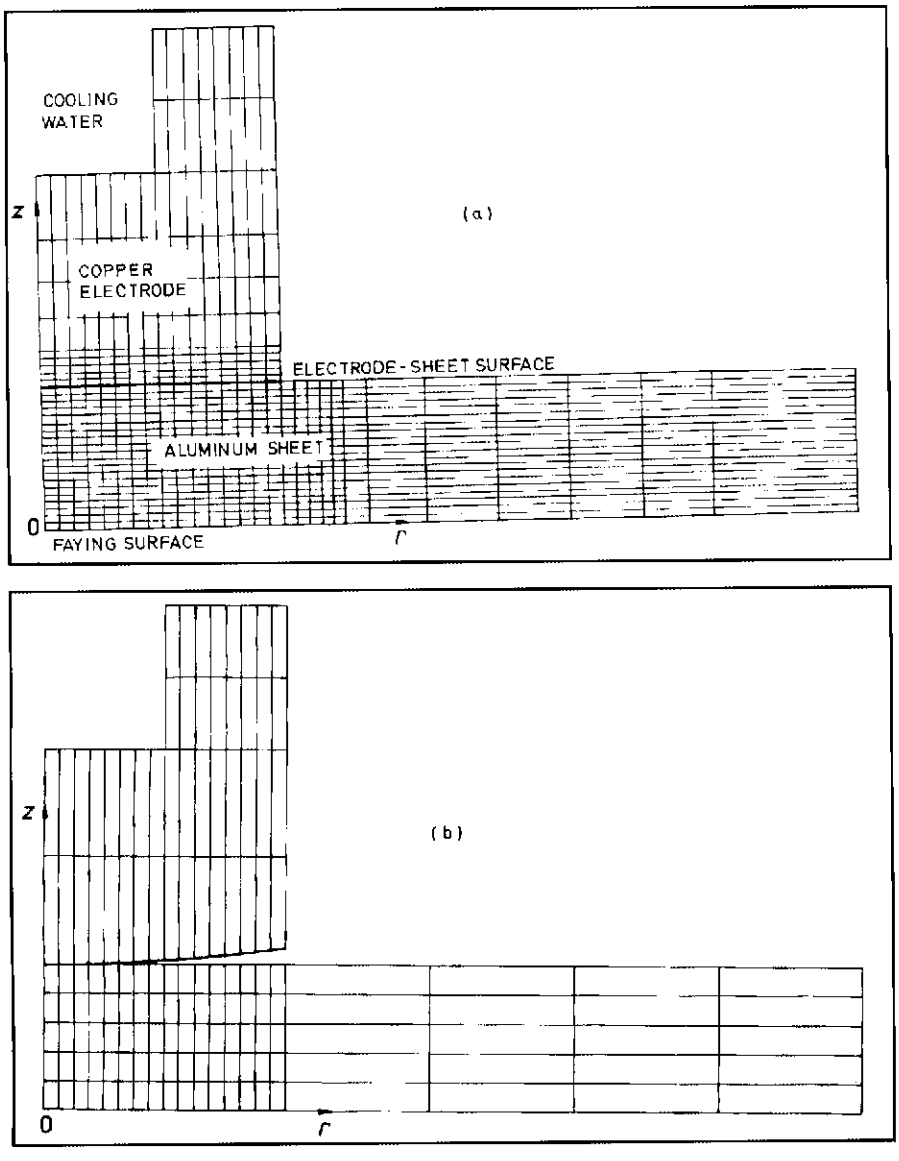

Fig. 1 — A — Mesh used in the finite difference module (electrothermal aspects); B — mesh used in the finite element module (deformation aspects).

this work.

Considerable advances have been made in modeling resistance spot welding, and the application of modeling to ferrous alloys gives rise to the possibility of improved process control (Refs. 7–9). However, existing models incorporating mechanical deformation have simulated spot welding with flat-ended electrodes and have not taken into account the change in contact area that accompanies welding with domed electrodes. This may not be a serious limitation in simulating welding in steel, but it may be more important in the study of spot welding of aluminum alloys where contact resistance at the faying surface is a dominant variable. It is the purpose of this paper to describe the development of a model of resistance spot welding applied to aluminum alloys, which is able to take into account the sensitivity of nugget formation in aluminum to the value of the faying surface resistance and area of contact at the faying surface. Such a model can be used to investigate the interaction of variables on fusion and nugget formation to determine the relative effect of critical process parameters.

The Model

The axisymmetric arrangement shown in Fig.1 was assumed for ease of computation. The sequence of events during a spot welding cycle can be separated into the following stages:

1) A force P is applied to the electrodes, which produces elastic and plastic deformation in the sheets. The deformation results in different areas of contact at the electrode-sheet surface and at the faying surface, the size of which depends on the applied force, the yield stress s_y of the aluminum and the Young's moduli of the sheet and the electrode.

2) At the start of the welding cycle, with the sheets and electrode at a uniform temperature T, current passes through the copper electrodes, flowing through the sheets and faying surface contact in the process. Both the electrodes and the sheets have well-defined values of electrical and thermal conductivity (σ, k), which are initially constant. The contact resistance R_c at the faying surface is not well-defined and has to be specified with reference to experimental determinations, depending on the alloy and any coating it may possess. An important application of the model is to investigate the sensitivity of nugget formation to variations in R_c.

3) As a consequence of the current flow, at some short time δt after the start of current flow, the temperature will increase at a rate that depends on the local value of the resistance. At the same time heat will flow out of the sheet and electrode into the cooling water at a rate dependent on the local value of the thermal conductivity k and the local temperature gradients. The distance between the electrode-cooling water interface will have a strong influence on the rate of abstraction of heat and can be varied in the model.

4) The properties of the materials will change locally as a consequence of the local increase in temperature. Consequently, the yield stress s_y will fall and more deformation will occur, increasing the areas of contact between the electrode and the sheet and between the faying surfaces. At the same time both the electrical and thermal conductivity will decrease as a function of the local temperature increase. These changes will affect both the local rate of heating and the rate of local heat conduction away from the faying surface.

5) The competing processes of ohmic heating and heat conduction will eventually lead to a steady state where the rate of change of temperature at any point is zero. However, if the current is large enough, melting will occur before the steady state is achieved, first at the faying surface, and then in an increasing volume of material about the faying surface. Fusion will absorb heat, but both the electrical and thermal conductivities decrease discontinuously in the molten zone to offset this effect. If the fusion zone becomes too large relative to the

area of contact determined by the applied force, weld metal expulsion will occur.

An axisymmetric model incorporating the above features was developed. The mechanical aspects of the problem were treated using the finite element technique. The electrical and thermal aspects were treated using the finite difference technique. The programs were coded and run in separate modules in the initial stages. After testing, the modules were linked as described in more detail below.

Electrothermal Module

The flexibility and speed of the finite difference method in solving heat transfer problems was exploited in developing the electrical-thermal module. Expressed in continuum form, solution of the temperature field involves the solution of the differential equation

$$\rho c \frac{\partial T}{\partial t} = \frac{\partial}{\partial r}\left(k \frac{\partial T}{\partial r} \right) + \frac{k}{r}\frac{\partial T}{\partial r} + \frac{\partial}{\partial z}\left(k \frac{\partial T}{\partial z} \right) + \sigma(\nabla\varphi \cdot \nabla\varphi) \quad (1)$$

where ρ is the density, c is the heat capacity, T is the temperature, t is the time and k and σ are the thermal and electrical conductivities, respectively. The axisymmetrical coordinates are denoted by r, which is the radial distance measured from the center of the electrode, and z, which is the distance in the direction parallel to the central axis of the electrode. The material properties c, k and σ are functions of temperature as indicated above. The last term on the right side of Equation 1 represents the heating produced by the potential φ. Because σ is a function of temperature and because the problem incorporates a number of different regions (e.g., copper electrodes, aluminum sheet, surface layers) the heating term varies with position and temperature and must be calculated independently at each time step in the computation. The governing differential equation for the calculation of the electrical potential φ is

$$\frac{\partial}{\partial r}\left(\sigma \frac{\partial \varphi}{\partial r} \right) + \frac{\sigma}{r}\frac{\partial \varphi}{\partial r} + \frac{\partial}{\partial z}\left(\sigma \frac{\partial \varphi}{\partial z} \right) = 0 \quad (2)$$

In solving Equations 1 and 2 by a numerical method, the differentials are replaced by finite differences relating to the values of T and φ at neighboring nodes in the chosen mesh (Refs. 10–12). The result is two coupled sets of linear equations. The set of equations arising from Equation 1 was solved numerically using the alternating direction implicit (ADI) method, which is well-documented in the literature (Refs. 10, 11). The method was chosen because it offers a stable solution for any choice of time step, and although the technique requires two solutions to be made in each time step, a tri-diagonal matrix is obtained so that each solution can be obtained using simplified Gaussian elimination. The instantaneous potential field defined in Equation 2 was solved by the successive overrelaxation method (Refs. 5, 10, 12). Because of the symmetry of the electrode pair, only one quarter of the physical arrangement need be modeled with a mesh of the sort shown in Fig. 1A. The total simulated time for completion of the spot welding cycle was of the order of 0.2 s, and solutions for the temperature and potential fields were obtained after each time step of 2×10^{-4} s. The source code to accomplish this was written in Fortran (Ref.13) and initially compiled in a Sun Sparkstation operating under Unix Sun OS. Subsequently, the code was transferred to a Cray operating under Unix.

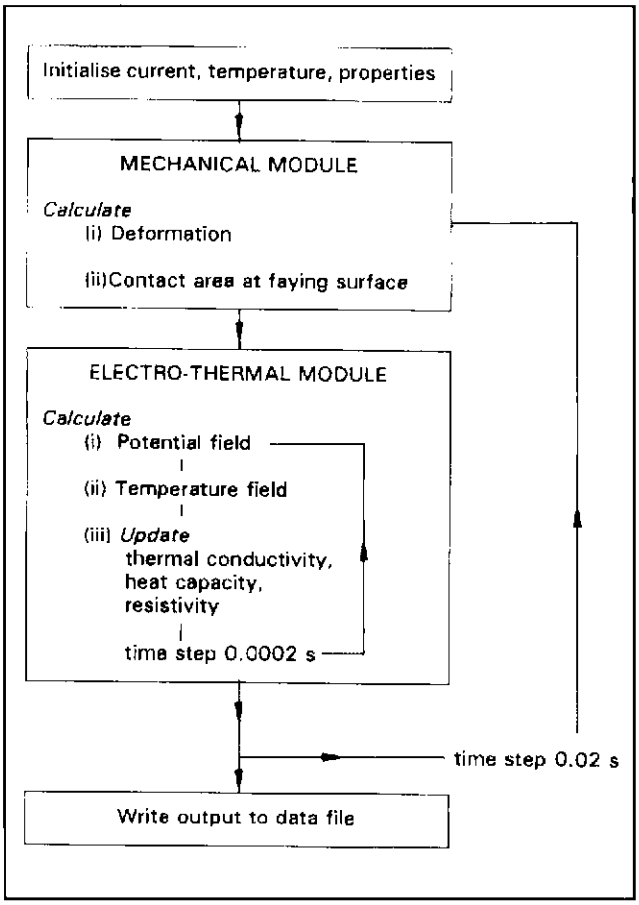

Fig. 2 — Schematic illustration of computational procedure.

The mechanical deformation affects the electrothermal process through its effect on the areas of the contacting surfaces. This was simulated in the model by passing the temperature field to the finite element module, called as an external procedure at intervals of 0.02 s (simulated time). The updated contact areas were then passed back to the electrothermal module from the finite element module, as shown schematically in Fig. 2. This frequency of linkage was found to be sufficient to monitor the significant changes in the areas of contact during the spot welding cycle.

Mechanical Module

The axisymmetric mechanical deformation was modeled with the finite element method, using the mesh of four-node, isoparametric elements shown in Fig. 1B. Plastic deformation was modeled using the von Mises isotropic yield criterion (Ref. 14) in which Young's modulus E, Poisson's ratio ν, yield stress s_y and work hardening rate h are the specified materials parameters. Provision was made in the module for incorporating the temperature dependence of the yield stress (empirical data), which falls significantly as the temperature increases. Solution of the finite element problem involves the solution of a system of simultaneous equations of the form

$$H\Phi + f = 0 \quad (3)$$

where Φ is the vector of unknown displacements, f is the vector of "loads" and H is the "stiffness matrix" (Ref. 15). For the elasto-plastic problem, H itself depends on the unknowns Φ so that an iterative method of solution was used, based on a modified Newton-Raphson method. This method was implemented in source code written in Fortran (Ref. 16) and designed to interface with the electrothermal module. The object code was initially compiled in a Sun Sparkstation under Sun OS. Subsequently, the code

Table 1 — Default Values of Variables

Variable	Default Value
Input Current (50 Hz sine wave)	20 kA
Contact Resistance	450 μΩ
Cooling Water-Tip Distance	3 mm (0.12 in.)
Applied Force	5 kN (1120 lb-force)
Sheet Thickness	2 mm (0.08 in.)
Electrode Tip Radius	50.8 mm (2 in.)

was transferred to a Cray operating under Unix.

The linked object code from the electrothermal and mechanical modules was run initially under Unix on a Sun Sparkstation and, typically, a full simulation of one welding cycle (0.16 s) took two hours to complete. The code was subsequently transferred to a Cray under Unix.

Parameters and Boundary Values

As with any numerical model, it is of great importance to define the boundary conditions and material parameters correctly to obtain realistic results. However, the exact values of some parameters are not known. In these cases test solutions can be made to determine the sensitivity of the final result to variations in the parameters in question. As described below, of the parameters with uncertain values, only the faying surface contact resistance was problematical. The boundary conditions used in the model are now described:

Thermal Boundary Conditions. The temperature of the cooling water, electrode and aluminum sheets was initialized at 20°C (68°F). Initial studies of the process showed that convective heat transfer to the surrounding air is negligible and can be ignored in the problem. To simulate the effect of a good flow of cooling water in the electrode cavity the temperature of the electrode-water interface was maintained at a constant value during the welding cycle.

Electrical Boundary Conditions. To drive the current, the potential at the top of the copper electrode was set to unity and the potential at the base of the mesh, at the faying surface was set to zero. These values were then scaled at each time step in accordance with the peak input current selected and the shape of the predetermined current pulse. For the simulations reported below, a 50 Hz sine wave current pulse was used.

Mechanical Boundary Conditions. On the base of the mesh, at the faying surface, the vertical displacement can only be zero or positive since the two surfaces can part but not overlap. It was found that no significant tangential stresses develop over the area of physical contact at the faying surface. Hence, the question of appropriate constraints in the radial direction does not arise in this case. In contrast, stresses tangential to the interface are found to develop at the electrode-sheet surface, indicating the possibility of sliding, depending on the coefficient of friction. To simplify the analysis, sliding at the electrode-sheet interface was not modeled, which is equivalent to assuming a large friction coefficient. The predetermined, constant applied force was maintained by adjusting the displacement. The yield strength at room temperature was taken to be 158 MPa (23 ksi) and the variation of yield strength with temperature was included using experimental data for AH 5754 aluminum alloy (Ref. 17). Full modeling of melting in its effect on mechanical deformation is very difficult because of the change in phase, which the finite element method is not well adapted to handle. To simulate the effect of melting within the constraints of the numerical method, the Poisson's ratio of the material in the region at temperatures above the melting point was made to be close to 0.5 and the shear yield strength was made small (10 MPa; 1.5 ksi) as was compatible with producing a stable solution. Ideally, Poisson's ratio should be set to a value of 0.5 to represent a liquid, but finite element models cannot generally handle this limiting case. In the present work, Poisson's ratio was set to 0.485 to model the liquid region.

Material Properties. Data for specific heat and electrical and thermal conductivities as a function of temperature (Refs. 18–20) were included in the data input file, and the values used in the model were updated at each time step. The extreme in the specific heat capacity at the melting point was incorporated using isothermal absorption of the fusion energy.

Contact Resistance. Boundary nodes not in physical contact with the electrode or at the faying surface (zero normal pressure at that point) were treated as insulating by assigning an effectively infinite resistance to them. An increase in the contact area with time was modeled by assigning a finite resistance to the nodes that had come into contact since the end of the previous time step. The contact resistance at the electrode-sheet interface was ignored because experimental measurement has shown it to be low compared with the faying surface contact resistance (Ref. 21) and also because preliminary modeling studies showed that local melting at the electrode surface had very little effect on nugget formation. Contact resistance at the faying surface was incorporated in the model by the inclusion of nodes with a high resistivity at the area of contact at the faying surface. In the results reported below, it was assumed that the contact resistance was spatially uniform across the contact area at a given applied force. Contact resistance is anticipated to fall with increasing temperature and detailed information on this effect in steel is available (Refs. 22–24). However, experimental observations show that the contact resistance at the faying surface in coated aluminum alloys remains reasonably constant until the temperature is close to the melting point (Ref. 21). Although it is easy to model detailed variations in the contact resistance with temperature and current flow using the present software, the following procedure was adopted for heuristic purposes. The contact resistance was maintained constant until the temperature at faying surface nodes exceeded the solidus temperature of the aluminum alloy. The contact resistance was then allowed to drop to the level of that of the molten metal over a temperature range of 50°C (122°F), which corresponds approximately to the solidus-liquidus range in aluminum alloys of interest.

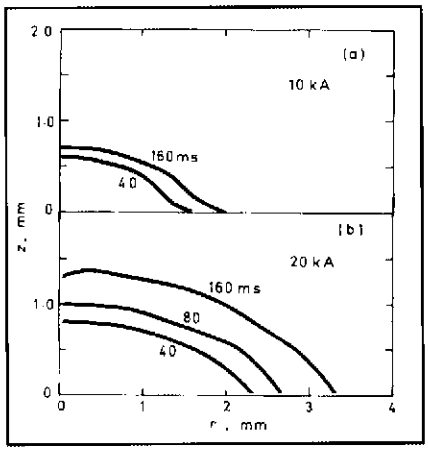

Fig. 3 — Nugget profiles (boundary between molten and solid metal) developed at different times in the welding cycle. The effect of different input currents (sinusoidal wave form) is shown with: A — input current of 10 kA (peak); B — current of 20 kA (peak). Other variables are set to the default values shown in Table 1.

Results of Simulations

Some simulations were performed to observe the effect of various parameters

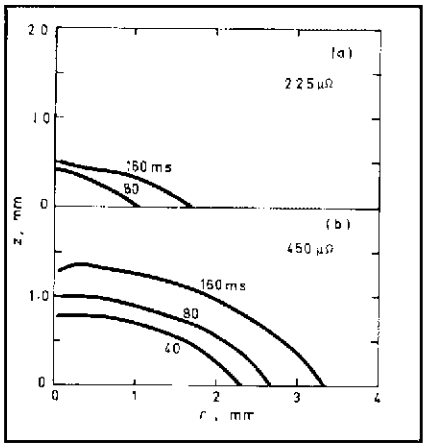

Fig. 4 — Nugget profiles developed at different times in the welding cycle showing the effect of contact resistance. A — 225 μΩ; B — 450 μΩ.

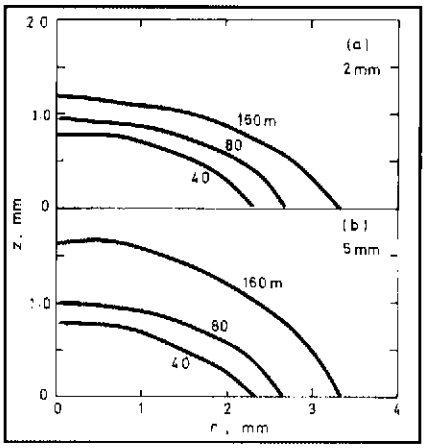

Fig. 5 — Nugget profiles developed at different times in the welding cycle showing the effect of the position of the cooling water from the electrode tip. A — 2 mm; B — 5 mm.

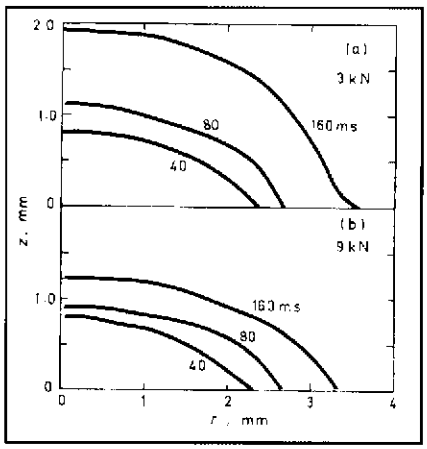

Fig. 6 — Nugget profiles developed at different times in the welding cycle showing the effect of the applied force. A — 3 kN; B — 9 kN.

on nugget formation. Unless stated otherwise, the default values listed in Table 1 were adopted. The effect of input current on nugget formation is shown in Fig. 3. In reasonable agreement with experience of resistance spot welding of aluminum, a current of 10 kA is found to be insufficient to form a good size nugget, whereas 20 kA is adequate, *i.e.*, the current values required for the resistance spot welding of aluminum are about three times larger than for steel owing to the higher electrical and thermal conductivity of the material.

The input current is a primary control variable in spot welding, but resistance spot welding of aluminum is expected to be sensitive to the value of the contact resistance at the faying surface, which in practice can vary between wide limits depending on the thickness of the oxide film and any coating applied to the material (Ref. 18). The range of values of the contact resistance used in the simulations was selected on the basis of experimental observations (Ref. 18). The results of simulations (Fig. 4A and B) illustrate the importance of the faying surface contact resistance. A factor of two decrease in the value of the contact resistance has the effect of reducing the local heating at the contacting surfaces sufficiently to suppress nugget growth. This result contrasts with the result of spot welding simulations done on steel using the present model (Ref. 25), which show that the value of the contact resistance is not such a critical factor in spot welding steel as in aluminum.

Because of the high thermal conductivity of aluminum the distance between the electrode-cooling water interface and the electrode tip has a significant effect on spot welding. As illustrated in Fig. 5, too much heat may be abstracted from the weld region to form a good-sized nugget when the distance is small. When the distance is large, a larger nugget is formed, although unwanted melting is then likely to occur at the electrode-sheet interface, with a consequent reduction in electrode tip life (Ref. 26).

The main effect of increasing the applied force is to increase the contact area and reduce the current density. In addition, because of its sensitivity to contact resistance, nugget formation is expected to be sensitive to the contact area at the faying surface, which in turn is determined by the applied force. With a low applied force of 3 kN, a large, round nugget is formed. With an applied force of 9 kN, a much flatter nugget is formed as a consequence of the lower current density at the center of the weld — Fig. 6.

Discussion

The development of an integrated electro-thermal-mechanical model has allowed the realistic modeling of resistance spot welding of aluminum to be undertaken. In particular, the incorporation of mechanical deformation in the model enabled the contact area at the faying surface to be included in the computation, to account for the change in contact area as temperature rises. The modeling of mechanical deformation is also envisaged to be useful in studies of the effect of applied force on molten metal expulsion at the faying surface, and the results of a study of this is presented in a separate publication (Ref. 27). The results presented in the present work show that the effect of a number of variables and their interaction can be readily studied and confirm previous findings that the contact resistance is crucial in spot welding aluminum, in contrast to the spot welding of steel. This raises a problem in the application of simulation to the study of spot welding in production because the contact resistance at the faying surface is the least understood and least controllable of all the parameters incorporated into the model.

The contact resistance of aluminum alloys is likely to be determined by both the roughness of the surface and the thickness of oxide films and any coating that has been applied to the sheet. It is often assumed that the deformation of surface asperities during compression of the faying surface largely determines the value of the contact resistance at the faying surface (*e.g.*, Ref. 9), but experimental work (Ref. 21) has shown that this may not always be the case at the faying surface in aluminum alloys, particularly when the sheet has been coated with an insulating film. Hence, an important use for simulation by computer modeling is to obtain a better understanding of the least understood aspects of the process, such as the role of the contact resistance and the details of the breakdown of contact resistance during melting.

Various patterns of possible behavior of contact resistance can be investigated inexpensively using the model. However, for this to be realistic and useful, the boundary conditions must be appropriate to spot welding in practice and take account of the effect of previously-formed spot welds, which form a shunt in the electrical circuit during the weld cycle. It is a relatively simple matter to incorporate a shunt resistance in to the model, but the effect of the presence of the shunt induces more complex behav-

ior. For instance, given the assumptions built into the simulations reported above, a high contact resistance is beneficial when no shunt is present, but may not be when there is a shunt resistance because of the diversion of current away from the weld. A study of the interaction between contact resistance and the presence of shunt welds and other factors using the present model is presented in a separate publication (Ref. 27).

Conclusions

1) A model of resistance spot welding of aluminum has been made incorporating the electrical, thermal and mechanical aspects of the process.

2) A primary effect of the applied force and mechanical deformation on nugget formation is the determination of the contact area and current density at the faying surface.

3) Preliminary studies of the effects of a number of variables on nugget formation are in good agreement with expectations, but a further development is to adapt the model to a more detailed study of resistance spot welding under production conditions which would include, for example, the effect of previously formed shunt welds. The results of a more detailed study of the influence of process variables will be presented in another paper (Ref. 27).

Acknowledgments

Grateful acknowledgment is made of the fact that two of the authors (D. Browne and J. Wen) were supported by Alcan International Ltd. in the period when this work was done. The authors also wish to acknowledge permission from Alcan International to publish this paper.

References

1. Archer, G. R. 1960. Calculations for temperature response in spot welds. *Welding Journal* 39(8): 327-s to 330-s.

2. Rice, W., and Funk, E. J. 1967. An analytical investigation of the temperature distributions during resistance welding. *Welding Journal* 46(4): 175-s to 186-s.

3. Gould, J. E. 1987. An examination of nugget development during spot welding, using both experimental and analytical techniques. *Welding Journal* 66(1): 1-s to 10-s.

4. Smith, R. A. 1980. Sizing of spot welds by elastic/plastic analysis. *Fracture and Fatigue*. Pergamon Press, pp. 49–56.

5. Cho, H. S., and Cho, Y. J. 1989. A study of the thermal behavior in resistance spot welds. *Welding Journal* 68(6): 236-s to 244-s.

6. Han, Z., Orozco, J., Indacochea, J. E., and Chen, C. H. 1989. Resistance spot welding: a heat transfer study. *Welding Journal* 68(9): 363-s to 371-s.

7. Nied, H. A. 1984. The finite element modeling of the resistance spot welding process. *Welding Journal* 63(4): 123-s to 132-s.

8. Kim, E., and Eager, T. W. 1990. Controlling parameters in resistance welding. *Sheet Metal Welding Conf., IV*. Paper 17.

9. Tsai, C. L., Dai, W. L., Dickinson, D. W., and Papritan, J. C. 1991. Analysis and development of a real-time control methodology in resistance spot welding. *Welding Journal*. 69(12): 339-s to 351-s.

10. Croft, D. R., and Lilley, D. G. 1977. *Heat Transfer Using Finite Difference Equations*. Applied Science Publishers Ltd., London, U.K.

11. Gerald, C. F., and Wheatley, P. O. 1989. *Applied Numerical Analysis*. Addison-Wesley Publishing Company, Reading.

12. Mitchell, A. R. 1969. *Computational Methods in Partial Differential Equations*. John Wiley and Sons, London, U.K.

13. Browne, D. J. 1992. Unpublished results, University of Newcastle upon Tyne, U.K.

14. Von Mises, R. 1928. Mechanik der plastischen formanderung der kristallen. *Z. Angew Math. Meth.* 8, pp. 161–246.

15. Zienkiewicz, O.C., Vallipan, S., and King, I. P. 1969. Elastoplastic solution of engineering problems: Initial stress, finite element approach. *Int. J. Num. Meth. Eng.* 1, pp. 75–176.

16. Wen, J. 1994. Mixed finite element analysis with application to spot welding, Ph.D. thesis, Newcastle upon Tyne, U.K., University of Newcastle upon Tyne.

17. Newton, C. J. 1992. Private communication, Alcan International, Banbury U.K.

18. Touloukian,Y. S., and Buyco, E.H. 1970. *Thermophysical Properties of Matter: Specific Heat*. Plenum, New York, N.Y.

19. Touloukian, Y. S., Powell, R. W., Ho, C. Y., and Klemens, P.G. 1970. *Thermophysical Properties of Matter: Thermal Conductivity*. Plenum, New York, N.Y.

20. Kaye, G. W. C., and Laby, T. M. 1986. *Tables of Physical and Chemical Constants*. Longman, London, U.K.

21. James, P. S. 1995. Electrical contact resistance: observations relevant to the spot welding of aluminium alloys, Ph.D. thesis. Newcastle upon Tyne, U.K., University of Newcastle upon Tyne.

22. Vogler, M. M. 1992 Investigation of spot welding formation, Ph.D. thesis, Stanford University.

23. Vogler, M. M. and Sheppard, S. D. 1992. A study of temperature histories in resistance spot welding. *The 3rd International Conference on Trends in Welding Research*, pp. 57–61, Gatlingburg, Tenn.

24. Vogler, M. M. and Sheppard, S. D. 1993. Electrical contact resistance under high loads and elevated temperatures. *Welding Journal*, 72(6): 1993 231-s to 238-s.

25. Browne, D. J., Chandler, H. W., and Evans, J. T. 1992. Unpublished results, University of Newcastle upon Tyne.

26. Patrick, E. P., Auhl, J. R., and Sun, T. S. 1984. Understanding the process mechanisms is key to reliable resistance spot welding aluminum autobody components. SAE paper 840291.

27. Browne, D. J., Chandler, H. W., Evans, J. T., James, P. S., Wen, J., and Newton C. J. 1992. Computer simulation of resistance spot welding in aluminium: part II. To be published.

Correction:

Re: Numerical Simulation of the Effect of Gravity on Weld Pool Shape, by J. Domey, D. K. Aidun, G. Ahmadi, L. L. Regel and W. R. Wilcox, pp. 263-s to 268-s, August 1995. The last paragraph on p. 266 reads in part, "This is evident in comparing the Grashof numbers for the 0.1- and 2.0-g cases which are 2.08 x 106 and 1.56 x 108, repectively." The numbers should read: 2.08×10^6 and 1.56×10^8.